

This is the peer reviewed version of the following article: Feigl, G., Kolbert, Z., Lehotai, N., Molnár, Á., Ördög, A., Bordé, Á., Laskay, G., Erdei, L. (2016). Different zinc sensitivity of *Brassica* organs is accompanied by distinct responses in protein nitration level and pattern. *Ecotoxicology and environmental safety*, 125, 141-152., which has been published in final form at <http://dx.doi.org/10.1016/j.ecoenv.2015.12.006>. This article may be used for non-commercial purposes in accordance with the terms of the publisher.

Title: Different zinc sensitivity of *Brassica* organs is accompanied by distinct responses in protein nitration level and pattern

Gábor Feigl*, Zsuzsanna Kolbert*, Nóra Lehotai, Árpád Molnár, Attila Ördög, Ádám Bordé,
Gábor Laskay, László Erdei

Department of Plant Biology, Faculty of Science and Informatics, University of Szeged,
Szeged – 6726 Közép fasor 52, Hungary

*These authors contributed equally to this work.

Corresponding author: Zsuzsanna Kolbert

e-mail: kolzsu@bio.u-szeged.hu

telephone/fax: +36-62-544-307

ABSTRACT

Zinc is an essential microelement, but its excess exerts toxic effects in plants. Heavy metal stress can alter the metabolism of reactive oxygen (ROS) and nitrogen species (RNS) leading to oxidative and nitrosative damages; although the participation of these processes in Zn toxicity and tolerance is not yet known. Therefore this study aimed to evaluate the zinc tolerance of *Brassica* organs and the putative correspondence of it with protein nitration as a relevant marker for nitrosative stress. Both examined *Brassica* species (*B. juncea* and *B. napus*) proved to be moderate Zn accumulators; however *B. napus* accumulated more from this metal in its organs. The zinc-induced damages (growth diminution, altered morphology, necrosis, chlorosis, and the decrease of photosynthetic activity) were slighter in the shoot system of *B. napus* than in *B. juncea*. The relative zinc tolerance of *B. napus* shoot was accompanied by moderate changes of the nitration pattern. In contrast, the root system of *B. napus* suffered more severe damages (growth reduction, altered morphology, viability loss) and slighter increase in nitration level compared to *B. juncea*. Based on these, the organs of *Brassica* species reacted differentially to excess zinc, since in the shoot system modification of the nitration pattern occurred (with newly appeared nitrated protein bands), while in the roots, a general increment in the nitroproteome could be observed (the intensification of the same protein bands being present in the control samples). It can be assumed that the significant alteration of nitration pattern is coupled with enhanced zinc sensitivity of the *Brassica* shoot system and the general intensification of protein nitration in the roots is attached to relative zinc endurance.

Key words: *Brassica juncea*, *Brassica napus*, protein tyrosine nitration, reactive nitrogen species, reactive oxygen species, zinc tolerance

1. INTRODUCTION

Zinc is typically the second most abundant metal in organisms after iron (Fe) and ~9% of the eukaryote proteome contains zinc (Andreini and Bertini 2009) suggesting its fundamental role in physiological processes. Indeed, zinc is involved in protein synthesis and in carbohydrate, nucleic acid, lipid metabolism and it is the only metal represented in all six enzyme classes (oxidoreductases, hydrolases, transferases, lyases, isomerases, ligases) (Broadley et al. 2007). Despite its necessity, at supraoptimal concentrations zinc can explicate phytotoxic effects as well. Generally, agricultural soils contain 10-300 $\mu\text{g Zn g}^{-1}$; however the Zn content of the soils can be enhanced by natural and anthropogenic activities including mining, industrial and agricultural practices. The pollution of soil by zinc has been a major environmental concern (Zarcinas et al. 2004). In non-tolerant plants, zinc toxicity occurs above 100-300 mg/kg dry weight tissue concentration. Toxic symptoms at the whole plant level involve reduced germination rate and biomass production (Munzuroglu and Geckil 2002), chlorosis, necrosis (Ebbs and Uchil 2008), loss of photosynthetic activity (Shi and Cai 2009), genotoxicity and disturbances in macro-and microelement homeostasis (Jain et al. 2010). Excess Zn may affect photosynthesis at different sites, including, *inter alia*, photosynthetic pigments, photosynthetic electron transport, RubisCo activity (Krupa and Baszynski 1995). At cellular level, zinc toxicity materializes through oxidative stress-associated lipid peroxidation, causing membrane destabilization in the plasmalemma, mitochondrial and photosynthetic membranes as well (Rout and Das 2003).

The non-redox active zinc has the ability to bind tightly to oxygen, nitrogen or sulphur atoms, hereby inactivating enzymes by binding to their cysteine residues (Nieboer and Richardson 1980). Also, zinc is able to cause secondary oxidative stress by replacing other essential metal ions in their catalytic sites (Schützendübel and Polle 2002). During zinc-triggered oxidative stress, reactive oxygen species (ROS), such as superoxide anion (O_2^-),

hydrogen peroxide (H_2O_2), and hydroxyl radicals ($\cdot\text{OH}$) are commonly generated as it was revealed by several authors (e.g. Morina et al. 2010; Jain et al. 2010). The level of ROS is needed to be strictly regulated by complex mechanisms in plants (Apel and Hirt 2004). These include several enzymes such as ascorbate peroxidase (APX, EC 1.11.1.11), glutathione reductase (GR, EC 1.6.4.2), catalase (CAT, EC 1.11.1.6) superoxide dismutase (SOD, EC 1.1.5.1.1), and non-enzymatic, soluble antioxidants such as glutathione and ascorbate, among others. The activity of several antioxidant enzymes and antioxidant contents was shown to be affected by zinc (Cuypers et al. 2002; Di Baccio et al. 2005; Tewari et al. 2008; Li et al. 2013).

Besides ROS, reactive nitrogen species (RNS) are also formed as the effect of wide variety of environmental stresses. The accumulation of these nitric oxide (NO)-related radicals and non-radical molecules (e.g. peroxynitrite, ONOO^- , S-nitrosoglutathione, GSNO) leads to nitrosative stress during which one of the principle post-translational modifications is tyrosine nitration in proteins yielding 3-nitrotyrosine (Corpas et al. 2013). During this peroxynitrite-catalyzed reaction an addition of a nitro group to one of the two equivalent ortho carbons in the aromatic ring of tyrosine residues (Gow et al. 2004) takes place causing steric and electronic perturbations, which modify the tyrosine's capability to function in electron transfer reactions or to keep the proper protein conformation (van der Vliet et al. 1999). In most cases nitration results in the inhibition of the protein's function (Corpas et al. 2013). Furthermore, tyrosine nitration has the ability to influence several signal transduction pathways through the prevention of tyrosine phosphorylation (Galetskiy et al. 2011).

Although oxidative stress triggered by heavy metals is well characterized in different plant species, until today, very little is known about heavy metal-, particularly essential element excess-induced nitrosative processes such as alterations in RNS metabolism and tyrosine nitration. Therefore, the main goal of this work was to evaluate and compare the ROS-RNS metabolism and the consequent protein nitration in the root and shoot system of two

76 economically important and moderately zinc accumulator plants (Ebbs and Kochian 1997),
77 Indian mustard (*Brassica juncea*) and oilseed rape (*Brassica napus*) exposed to prolonged zinc
78 excess. Furthermore, the determination of possible correspondence between the changes in
79 protein nitration and zinc tolerance was also a relevant issue of this study.

80

2. MATERIALS AND METHODS

2.1. Plant material and growth

Seeds of Indian mustard (*Brassica juncea* L. Czern. cv. Negro Caballo) were obtained from the Research Institute for Medicinal Plants of Budakalász, Hungary and the oilseed rape (*Brassica napus* L.) seeds from the Cereal Research Non-Profit Ltd. of Szeged, Hungary. The seeds of both species were surface-sterilized with 5% (v/v) sodium hypochlorite and then placed onto perlite-filled Eppendorf tubes floating on full-strength Hoagland solution where they grew for nine days. The nutrient solution contained 5 mM Ca(NO₃)₂, 5 mM KNO₃, 2 mM MgSO₄, 1 mM KH₂PO₄, 0.01 mM Fe-EDTA, 10 µM H₃BO₃, 1 µM MnSO₄, 5 µM ZnSO₄, 0.5 µM CuSO₄, 0.1 µM (NH₄)₆Mo₇O₂₄ and 10 µM AlCl₃. The nine-day-old seedlings were treated with 50, 150 or 300 µM ZnSO₄ for additional fourteen days. During the whole experimental period, the control plants were kept in full strength Hoagland solution containing 5 µM ZnSO₄. The plants were grown in a greenhouse at a photon flux density of 150 µmol m⁻² s⁻¹ (12/12h light/dark cycle) at a relative humidity of 55-60% and 25±2°C.

All chemicals used during the experiments were purchased from Sigma-Aldrich (St. Louis, MO, USA) unless stated otherwise.

2.2. Element content analysis

The concentrations of microelements were measured by using inductively coupled plasma mass spectrometer (ICP-MS, Thermo Scientific XSeries II, Asheville, USA) according to Feigl et al. (2013). Root and shoot material were harvested separately and rinsed with distilled water. After the drying on 70°C for 48 hours and digestion of the plant material (digestion process: 6 ml 65% (w/v) nitric acid was added to the samples followed by 2 hours of

incubation; then 2 ml of 30% (w/v) hydrogen-peroxide was added then the samples were subjected to 200°C and 1600W for 15 min), the values of Zn and other microelement (Fe, Mn, B, Cu, Mo, Ni) concentrations were determined. The concentrations of Zn are given in mg/g dry weight (DW), while the concentrations of other microelements are given in µg/g DW.

2.3. Measurement of photosynthetic pigment composition

In the leaves of the control and Zn-treated *Brassica* species, the amount of chlorophyll *a*, *b* and total carotenoids were determined according to Lichtenthaler (1987). The calculated amounts of the pigments are expressed as µg pigment/g fresh weight.

2.4. Shoot morphological measurements

The fresh weights (FW) and the dry weights (DW) of the carefully separated shoot material were measured on the 14th day of the treatment using a balance. Leaf area was determined on at least 10 specimens in every case by using a grid and ImageJ software (National Institute of Mental Health, Bethesda, Maryland, USA).

2.5. Measurement of chlorophyll fluorescence parameters

Chlorophyll fluorescence parameters were measured using a Pulse Amplitude-Modulated Fluorometer (Program “Run 8”, PAM 200 Chlorophyll Fluorometer, Heinz Walz GmbH, Effeltrich, Germany). Leaves of treated and control plants were first dark adapted for 30 minutes and F_m , F_m' , F_t and F_o' parameters were measured in the function of increasing light intensity (PAR = Photosynthetic Active Radiation) from 60 to 850 µmol photons/m/s. From these parameters the effective quantum yield of PSII (Yield = $(F_m' - F_t)/F_m'$), electron transport rate (ETR = Yield x PAR x 0.5 x 0.84), photochemical quenching (qP = $(F_m' - F_t)/(F_m' - F_o')$) and non-photochemical quenching (NPQ = $(F_m - F_m')/F_m'$) were calculated and

recorded. All measurements were carried out on leaves from five different plants in three parallel experiments.

2.6. Root morphological measurements

The length of the primary root (cm) and the first six lateral roots from the root collar (cm) were determined manually. Also the visible lateral roots were counted and their number is expressed as pieces/root.

2.7. Detection of viability loss, reactive oxygen- (ROS) and nitrogen species (RNS) in the root tissues

In all cases, approx. two cm-long segments were cut from the root tips and these were incubated in 2 mL dye/buffer solutions in Petri-dishes with 2 cm diameter. After the staining procedure, the root samples were prepared on microscopic slides in buffer solution.

The viability of the root meristem cells was determined using 10 μ M fluorescein diacetate (FDA) solution (in 10/50 mM MES/KCl buffer, pH 6.15) at room temperature (25 \pm 2°C) in the dark (Lehotai et al. 2012).

The level of superoxide anion in the root tip was estimated using 10 μ M dihydroethidium (DHE) (prepared with 10 mM Tris/HCl, pH 7.4) in the dark at 37°C. (Kolbert et al. 2012).

For hydrogen peroxide detection, root tips were incubated in 50 μ M AmplifluTM (10-acetyl-3,7-dihydroxyphenoxazine, ADHP or Amplex Red) solution at room temperature in the dark for 30 minutes according to Lehotai et al. (2012).

The fluorophore, 4-amino-5-methylamino-2',7'-difluorofluorescein diacetate (DAF-FM DA, 10 μ M in 10 mM Tris/HCl buffer, pH 7.4) was applied for the visualization of NO levels in *Brassica* root tip segments (Kolbert et al. 2012).

For the *in situ* and *in vivo* detection of peroxynitrite (ONOO⁻), 10 μ M 3'-(*p*-aminophenyl) fluorescein (APF) was applied according to Chaki et al. (2009). Although these staining methods allow semi-quantitative determinations, they are reliable tools for *in situ* detection of ROS and RNS, since their specificity were proved *in vivo* and *in vitro* (Kolbert et al. 2012).

The roots of the plants labelled with different fluorophores were investigated under a Zeiss Axiovert 200M inverted microscope (Carl Zeiss, Jena, Germany) equipped with filter set 9 (exc.: 450-490 nm, em.: 515- ∞ nm) for DHE, filter set 10 (exc.: 450-490, em.: 515-565 nm) for APF, DAF-FM and FDA, filter set 20HE (exc.: 546/12, em.: 607/80) for Amplex Red. Digital photographs from the samples were taken by a digital camera (Axiocam HR, HQ CCD). The same camera settings were applied for each digital image. In all cases, fluorescence intensities (pixel intensity) in the meristematic zone of the primary roots were measured on digital images using Axiovision Rel. 4.8 software within circles of 100 μ m radii. At least 10-15 root tips were measured in each experiment.

2.8. Measurement of the enzymatic antioxidant activity and lipid peroxidation

The activity of superoxide dismutase (EC 1.15.1.1) was determined by measuring the ability of the enzyme to inhibit the photochemical reduction of nitro blue tetrazolium (NBT) in the presence of riboflavin, in light (Dhindsa et al. 1981). For the enzyme extract, 250 mg fresh plant material was grinded with 10 mg polyvinyl polypyrrolidone (PVPP) and 1 ml 50 mM phosphate buffer (pH 7.0, with 1 mM EDTA added). The enzyme activity is expressed in Unit/g fresh weight; one unit (U) of SOD corresponds to the amount of enzyme causing a 50% inhibition of NBT reduction in light.

Ascorbate peroxidase (APX; EC 1.11.1.11) activity was measured by monitoring the decrease of ascorbate content at 265 nm (ϵ =14 mM⁻¹ cm⁻¹) according to a modified method by

Nakano and Asada (1981). For the enzyme extract, 250 mg fresh plant material was grinded with 1.5 ml extraction buffer containing 1mM EDTA, 50mM NaCl and 900 μ M ascorbate. Data are expressed as activity (Unit/g fresh weight).

The zinc-induced lipid peroxidation in the root and shoot tissues was quantified by the measurement of thiobarbituric acid reactive substances (TBARS) concentration (Heath and Packer 1968). 100 mg of shoot and root tissues were freshly grounded in liquid nitrogen, suspended in 1 ml 0.1% tri-chloro acetic acid (TCA), and then centrifuged at 12.000 rpm for 20 min in the presence of butylated hydroxytoluene (BHT) (0.1 ml, 4%) to prevent further lipid peroxidation. 250 μ l of the supernatant was removed and incubated at 100°C for 30 min with 1 ml of 0.5% 2-thiobarbituric acid (TBA) dissolved in 20% TCA. After cooling the samples on ice, they were refilled to the starting volume. The absorbance of the supernatant was determined at 532 nm, and corrected for unspecific turbidity after subtraction from the value obtained at 600 nm. The level of lipid peroxidation is expressed as nmol TBARS per gram fresh weight, using an extinction coefficient of 155 mM⁻¹cm⁻¹.

2.9. SOD activity on native PAGE, isoform staining

The isoforms and activity of SOD (Mn-SOD, Fe-SOD, Cu/Zn-SODs) were detected in gel according to the modified method of Beauchamp and Fridovich (1971). After the separation of SOD isozymes by non-denaturing PAGE on 10% acrylamide gels, they were incubated sequentially in 2.45 mM NBT for 20 min and in 28 μ M riboflavin and 28 mM tetramethyl ethylene diamine (TEMED) for 15 min in the dark. After light exposure, the colourless SOD bands were observed on a dark blue background. The different isoforms were identified by incubating the gels in 50 mM potassium phosphate buffer (pH 7.0) supplemented with 3 mM KCN (inhibits Cu/Zn SOD) or 5 mM H₂O₂ (inhibits both Cu/Zn- and Fe-SOD) for 30 min before staining with NBT. Mn-SODs are resistant to both inhibitors.

2.10. Preparation of protein extract

Shoot and root tissues of *Brassica* species were grounded with double volume of extraction buffer [50 mM Tris-HCl buffer (pH 7.6-7.8) containing 0.1 mM EDTA (ethylenediaminetetraacetic acid), 0.1% Triton X-100 [polyethylene glycol p-(1,1,3,3-tetramethylbutyl)-phenyl ether) and 10% glycerol]. After centrifugation at 12,000 rpm for 20 min at 4°C, the supernatant was stored at -20°C. Protein concentration was determined using the Bradford (1976) assay with bovine serum albumin as a standard.

2.11. SDS-PAGE and Western blotting

10 µg of root and 25 µg of shoot protein extracts per lane were subjected to sodium dodecyl sulphate-polyacrylamide gel electrophoresis (SDS-PAGE) on 12% acrylamide gels. For western blot analysis, separated proteins were transferred to PVDF membranes using the wet blotting procedure (30 mA, 16 hours). After transfer, membranes were used for cross-reactivity assays with rabbit polyclonal antibody against 3-nitrotyrosine diluted 1:2000 (Corpas et al. 2008). Immunodetection was performed by using affinity isolated goat anti-rabbit IgG-alkaline phosphatase secondary antibody in dilution of 1:10 000, and bands were visualised by using NBT/BCIP reaction. As a positive control nitrated bovine serum albumin was used.

2.12. Statistical analysis

All experiments were carried out at least two times. The results are expressed as mean ± SE. Multiple comparison analyses were performed with SigmaStat 12 software using analysis of variance (ANOVA, P<0.05) and Duncan's test.

3. RESULTS AND DISCUSSION

3.1. Zinc accumulation and translocation capacity of *Brassica* species are similar

As the effect of increasing external zinc sulphate concentrations, the zinc content of the root system of both species dramatically increased (Fig 1a). The roots of *B. napus* showed maximal accumulation already at 150 μ M Zn, while in *B. juncea* roots, by 60% lower zinc concentration was measured at this treatment. This indicates that *B. napus* roots possess a more efficient zinc uptake system compared to *B. juncea*. Moreover, the enhancement of zinc concentration in the root tissues of *B. juncea* proved to be directly proportional to the external zinc concentration of the nutrient solution ($R^2=0.999$). In the aerial plant parts, as the effect of external exposure the zinc concentration significantly enhanced (Fig 1b) in both species, suggesting that root-to-shoot transport occurs. The most abundant transport forms of zinc are complexes with citric, malic and oxalic acid (Lu et al. 2013). According to the results of White et al. (1981), small amounts of soluble zinc-phosphate can also be found in the xylem sap of zinc stressed plants. However, it has to be noted that in the shoot tissues, an order of magnitude lower zinc contents were measured compared to the root. This suggests that the zinc translocation capability of the *Brassica* species is relatively poor, which can be a part of an exclusion defence strategy (Baker 1987). With the restriction of its root-to-shoot translocation, plants try to protect the more sensitive shoot from zinc-induced damages. At the same time, both species accumulated more zinc than 0.1% of the shoot dry weight (0.45% of shoot DW in *B. juncea* and 0.49% of shoot DW in *B. napus*); therefore both species are considered to be zinc accumulators. In other works, similar Zn accumulation tendencies were observed in the *Brassica* species, and they were considered to be as moderate zinc accumulators (Kumar et al. 1995, Ebbs et al. 1997; Ebbs and Kochian 1997).

3.2. Excess zinc induces similar disturbances in the microelement homeostasis of *Brassica* species

Besides zinc, the concentrations of iron (Fe), manganese (Mn), boron (B), copper (Cu), molybdenum (Mo) and nickel (Ni) were also measured by ICP-MS, in order to evaluate the putative disruption in microelement homeostasis provoked by zinc exposure (Supplementary Figure 1). Surprisingly, excess zinc led to the increase of copper content in both organs of both species. This can be explained by that both ions use the same transporters, which can be up-regulated by excess Zn, although they prefer Cu (Fraústo da Silva and Williams 2001) provoking the increase of Cu content in the Zn-exposed plants. The manganese concentration was found to be remarkably decreased in the organs of Zn-exposed *Brassica* species, which suggests an antagonistic relationship between the two ions. Similarly to our results, in the shoots of zinc-exposed *B. juncea* and *B. napus* cultivars and in the roots of *Lolium perenne* the Mn contents were significantly reduced (Ebbs and Kochian 1997; Monnet et al. 2001). Decrease in manganese content may due to competition of zinc with manganese for transport sites in the plasmalemma. The concentrations of iron and boron were differentially influenced by zinc treatment in the organs. A notable zinc-induced loss of Fe content was observed in the shoot tissues of both species. In the case of *B. juncea*, the concentration of Fe ion remarkably increased within the root system, but it was not modified in the roots of *B. napus*. The synergistic effect between iron and zinc observed in *B. juncea* roots suggests that this species may intensify their iron uptake into the root in order to compensate iron diminution in leaves. In *Arabidopsis* roots, excess Zn notably induced the expression of the ferric-chelate reductase gene (FRO2), which contributed to the intensification of Fe uptake (van de Mortel et al. 2006). Although, the inhibitory effect of excess zinc on the root-to-shoot Fe translocation was also evidenced e.g. in soybean, Japanese mint or *Picea abies* (Ambler et al. 1970; Misra and Ramani 1991; Godbold and Huttermann 1985), which may provide a possible explanation for the altered

Fe distribution between the organs of *B. juncea*. Excess zinc modified the concentration of B in the organs of both species as well, and within the shoot system, the enhancement of B content was worth mentioning. Similar synergism between boron and zinc was observed in mustard by Sinha et al. (2000). The increase of Mo contents was evident in the shoot of Zn-exposed *Brassica*, and it was not modified within the root system. Moreover, Zn exposure did not significantly altered Ni concentrations of the *Brassica* organs. The observed changes in microelement concentrations and distribution suggest that excess zinc is able to disrupt the homeostasis of micronutrients in the organs by interfering with their uptake, translocation and metabolism (Stoyanova and Doncheva 2002). We observed similar changes in the *Brassica* species, which supports the species-independent rather general nature of the zinc-triggered micronutrient disturbances.

3.3. Growth and morphology of *Brassica* organs are differentially affected by excess zinc

During control circumstances, the shoot system of *B. napus* proved to be more extended than that of *B. juncea*, which is indicated by the significantly higher fresh, dry biomass and the larger leaf area of it (Fig 2 a, b and c, respectively). As the effect of 50 and 150 μM Zn, concentration-dependent decrease of shoot FW was observed in both species (Fig 2a). The most serious Zn exposure (300 μM) did not reduce the biomass further compared to the 150 μM Zn treatment. Regarding the shoot DW (Fig 2a), Zn at all concentrations reduced it significantly compared to the control. In case of both fresh and dry biomass, the species were differentially affected, since in *B. juncea*, Zn resulted in 78% reduction of shoot FW and in 60% of shoot DW, but *B. napus* showed only 64% and 43% loss of shoot FW and DW, respectively.

The leaf area of both *Brassica* species was significantly reduced by all Zn concentrations (Fig 2b). Although, higher doses of Zn treatment (150 and 300 μM) caused by ~8% slighter leaf growth inhibition in *B. napus* compared to *B. juncea*.

In the two *Brassica* species, excess zinc significantly decreased chlorophyll (chl) *a*, *b* and carotenoid contents, although, the effects were more pronounced in *B. juncea* (Supplementary Table 1). As the effect of 300 μ M Zn, both total chlorophyll and carotenoid contents decreased more significantly in *B. juncea* leaves compared to *B. napus*. In *B. napus*, the rate of loss was greater in case of chl *b* compared to chl *a*, which resulted in the increment of chl *a/b* ratios suggesting that chl *b* pool is more sensitive to excess Zn than chl *a*. By Ebbs and Uchil (2008) two possible mechanisms were supposed for Zn-induced chlorophyll loss including the increased conversion of chl *b* to chl *a* contributing to the maintenance of the more important chl *a* pool under zinc stress. The other possible mechanism can be the metal-induced down-regulation of chl *a* oxygenase enzyme involved in chl *b* synthesis. Moreover, iron deficiency (see Supplementary Figure 1), or substitution of the central magnesium ion with Zn may also contribute to the observed Zn-triggered chlorophyll loss (Prasad and Strzalka 1999). Chlorosis can be associated also with Mn deficiency (Last and Bean 1991), which in our system can also be the reason of the chlorophyll diminution.

In Fig 2c and d, Zn-triggered changes in leaf morphology and chlorotic symptoms can be seen. On the leaf blades of *B. juncea*, also necrotic lesions can be observed (marked by arrows in Fig 2d) reflecting a serious damage induced by zinc in this species.

In order to get a more accurate view about the zinc-induced damage of the shoot system, chlorophyll fluorescence parameters were determined which provide a reliable method for assessing photosynthetic activity under stress conditions (Roháček et al. 2008). Exposure to excess Zn induced inhibition of photosynthesis especially in *B. juncea* (Fig 3), while the effect was much slighter in *B. napus* leaves. Interestingly, the Yield, ETR and qP parameters of *B. juncea* were not affected by 300 and 50 μ M Zn treatment remarkably, but they were the most seriously reduced by 150 μ M Zn (Fig 3a). The results indicate that excess Zn is an effective blocker of PSII function, especially in *B. juncea* leaves. Indeed, it has been demonstrated that

the mechanism of action is the displacement of Mg by Zn at the water splitting site in photosystem II (van Assche and Clijsters, 1986; Kupper et al. 1996). Moreover, Teige et al. (1990) suggested that the primary toxic action of Zn is the inhibition of ATP synthesis and therefore energy metabolism in plants. Another background mechanism of the photochemical activity loss during zinc toxicity can be the alteration of the inner structure and composition of the thylakoid membrane (Baszynski et al. 1988). In contrast to *B. juncea*, excess Zn did not result in obvious inhibition of the observed parameters (Yield, ETR, qP) in the leaves of *B. napus* (Fig 3b). However, NPQ was found to increase as the effect of zinc exposure in both species. In *B. juncea*, only 150 μ M Zn enhanced the NPQ parameter, while in *B. napus* all applied zinc concentrations increased the probability of dissipating the excess excitation energy via this alternative route. In our system, the photosynthetic activity well correlates with the iron deficiency-associated chlorosis, since zinc-treated *B. juncea* showed more intense biomass reduction, necrotic damages, chlorophyll loss and consequently more pronounced decrease in photosynthetic activity compared to *B. napus*. Therefore, we assume that the photosynthesis of *B. juncea* is more sensitive to zinc stress than that of *B. napus*.

In contrast to the shoot, the reducing effect of excess zinc on the fresh and dry weights of the root system proved to be independent from the applied concentrations (Fig 4a). In both species, the most serious diminution was observed in case of 150 μ M ZnSO₄ treatment; although this effect was statistically significant only in *B. juncea*, despite that the root of this species accumulated smaller amount of zinc from the solution than that of *B. napus* (see Fig 1a). This suggests the greater zinc sensitivity of *B. juncea* compared to *B. napus*. During the detailed examination of the root architecture, some interesting differences were observed between the species. In *B. napus*, the elongation of the primary root was significantly inhibited by 150 μ M Zn; however it was only slightly, but not significantly affected in *B. juncea* (Fig 4b). This difference can be explained by the higher Zn accumulation of *B. napus* roots (see Fig

1a). Regarding the lateral roots, excess zinc resulted in a remarkable and concentration-dependent shortening of them in both species (Fig 4c), which refers to the higher sensitivity of the newly formed laterals compared to the primary root. Interestingly, zinc at all concentrations significantly increased the lateral root number of *B. juncea*, while in *B. napus* the effect proved to be much slighter (Fig 4d). The accession of lateral root number induced by heavy metals was described as a symptom of stress-induced morphogenetic response (SIMR, Potters et al. 2009). Similarly to our results, LR-inducing effect of Zn in *Sesbania* species was reported by Yang et al. (2004). The changes in meristem cell viability showed correlation with the zinc-induced shortening of the PRs, which supports the fundamental role of meristem cell activity in root elongation. The viability loss was notable already in 50 and 150 μ M Zn-exposed roots of the species, but in *B. napus* the viability reduction (Fig 4e) as well as the PR shortening (Fig 4b) proved to be more pronounced. Zinc-triggered cell death in the root system was proved, *inter alia*, in rice (Chang et al. 2005).

3.4. Excess zinc triggers changes in the ROS and RNS metabolism of the root system

Fluorescent microscopic techniques were applied for detecting the possible zinc-induced changes in ROS (superoxide radical and hydrogen peroxide) and RNS (nitric oxide and peroxynitrite) levels of the root system. During control circumstances all fluorophores showed higher fluorescence intensities in *B. juncea* roots than in those of *B. napus*. As the effect of zinc exposure, superoxide level slightly decreased in *B. napus*, in a concentration-dependent manner, while in the root tips of *B. napus* 150 μ M zinc caused the most serious superoxide anion depletion (Fig 5a). In both species the level of H_2O_2 was remarkably enhanced by zinc; although the accumulation was more intense in *B. juncea* roots (Fig 5b). The highest H_2O_2 contents were detected in *B. napus* treated with 50 and 150 μ M zinc. All zinc concentrations significantly increased the NO levels in *B. juncea* (Fig 5c). In *B. napus*, the zinc-triggered NO

generation proved to be slighter, but the 150 μ M zinc exposure resulted in comparably high NO level. The possible mechanisms underlying Zn-induced NO formation may be diverse. According to Xu et al. (2010), Zn-triggered Fe-deficiency could lead to NO formation; although in our experiments, the Fe content of the root system did not decrease (see Supplementary Figure 1). Furthermore, in our earlier experiments, the activity of the major NO-producing enzyme, nitrate reductase, was not influenced by excess zinc in *Brassica* roots (Bartha et al. 2005). Instead, another possibility of NO production in this system is the transition metal-triggered decomposition of NO pools such as S-nitrosoglutathione (Smith and Dasgupta 2000) but this hypothesis is needed to be confirmed in the future. Nitric oxide reacts with superoxide anion yielding peroxynitrite (ONOO^-), a powerful oxidative and nitrosative agent (Arasimowicz-Jelonek and Floryszak-Wieczorek 2011). Regarding the peroxynitrite content, interestingly the higher zinc doses (150 and 300 μ M) reduced it in *B. juncea* roots (Fig 5d), which showed no correspondence to the observed changes in NO and superoxide levels (Fig 5c). In the background of the zinc-induced peroxynitrite diminution, the activation of putative decomposition pathways (e.g. ascorbic acid, flavonoids, peroxyredoxin, and glutathione reductase) can be supposed (Arasimowicz-Jelonek and Floryszak-Wieczorek 2011). In contrast, the peroxynitrite levels increased in *B. napus* roots (Fig 5d), in a concentration-dependent manner; however no correlation of this with superoxide levels was found (Fig 5a).

Zinc at all applied concentrations intensified the activity of SOD enzyme in the roots of the species; however the effects were not dependent on the zinc doses and the activation was more pronounced in *B. napus* (Fig 6a). Within the shoot system, similar tendencies were observed. The different SOD isoforms were separated by native PAGE and five activity bands were identified in the organs of both species (Fig 6b). In Fig 6b, a representative SOD activity gel from *B. napus* is shown. The uppermost band represented a Mn-SOD isoform, which activity decreased as the effect of increasing Zn concentrations in the roots. The diminution of

Mn-SOD activity can be explained by the reduced availability of manganese as previously showed in Supplementary Figure 1. The Fe-SOD isoform was only present in the control sample of *B. napus*; its activity was seriously reduced by the zinc treatments. The last three bands showed Cu/Zn-SODs, which showed a remarkable activation, especially in the roots, which was in correlation with the overall SOD activity (see Fig 6a). The intensification of Cu/Zn-SODs may be the result of the increment of the Zn and Cu contents triggered by zinc exposure (see Supplementary Figure 1). Contrary to our results, significantly reduced total SOD and isoenzyme activities were observed in rapeseed; although younger plants were subjected to more severe zinc stress than in our system (Wang et al. 2009). The activity of APX decreased as the effect of zinc exposure in both organs of both species (Fig 6c). Interestingly, the activity loss was more pronounced in the shoot system of the species (especially in *B. juncea*). These imply that the effect of zinc on antioxidant enzymes (at least SOD and APX) is dependent on the plant age, the duration and the intensity of stress treatment. The observed changes in the antioxidant enzyme activities could explain the alterations in the ROS levels, since the zinc-triggered activation of SOD and deactivation of APX can be responsible for the superoxide depletion and the H₂O₂ accumulation in the roots. Regarding the lipid peroxidation being a marker of oxidative stress, no obvious tendencies and intensification were observed in the shoot system of the species (Fig 6d). Only in *B. juncea* roots, a significant increase in the amount of lipid peroxides (e.g. TBARS) could be determined as the effect of all applied zinc concentrations.

3.5. Excess zinc induces changes in the level and the pattern of protein tyrosine nitration

Using Western blot analysis, the presence of several 3-nitrotyrosine-positive protein bands were detected in the untreated samples (Fig 7), which suggests that a part of the protein pool of the organs is nitrated even under control conditions. This raises the possibility that

tyrosine nitration is a basal regulatory mechanism of protein activity. Similarly, a basal nitration state of proteins was evidenced in different plant species such as sunflower, *Citrus*, pea and pepper (Chaki et al. 2009, Begara-Morales et al. 2013, Corpas et al. 2013, Chaki et al. 2015). Moreover, the protein pool of the shoot of both *Brassica* was more nitrated compared to the root system, where the 3-nitrotyrosine-positive signals were much weaker indicating the organ specificity of protein tyrosine nitration. In preliminary experiments, we did not observe concentration-dependent effect of zinc on the level of tyrosine nitration, therefore based on other data 150 μ M zinc was chosen for further analysis. In general, the pattern of protein nitration was modified by zinc in the shoot system of the species, while a general strengthening of 3-nitrotyrosine-associated immunopositivity was observed in the root system of the zinc-exposed species. Based on this, we can assume that the proteome of the *Brassica* organs are differentially affected by zinc-triggered nitration. In the shoot of *B. juncea*, the nitration of the protein bands at 50, 37 and \sim 12 kDa decreased, while two new, immunopositive bands appeared between 15 and 20 kDa. In the shoot of zinc-exposed *B. napus*, the tyrosine nitration of protein bands at 50, 37, 25 and \sim 12 kDa weakened, while a slight intensification was observed in two other protein bands suggesting the modification of nitration pattern of the organ. In contrast to the shoot, the nitration level of the root proteome of both species intensified as the effect of 150 μ M zinc; however, the response was much more intense in *B. juncea* roots. Similarly, the enhancement of the nitration levels was published, *inter alia*, in salt-stressed olive leaves, in cold-treated pea leaves or in arsenic-exposed *Arabidopsis* (reviewed by Corpas et al. 2013).

4. CONCLUSIONS

Among the two moderate Zn accumulator *Brassica* species, oilseed rape took up and translocated more zinc compared to *B. juncea*. Still the shoot of *B. napus* showed slighter zinc-induced damages (examined by growth and morphology parameters, pigment contents and photosynthetic activities), which were accompanied by the activation of antioxidants and the

moderate alteration of protein nitration pattern. Based on the examined parameters (PR length, LR number, viability) the root system of *B. juncea* showed enhanced tolerance to zinc exposure compared to *B. napus*, and it was coupled with enhanced H₂O₂, NO levels and remarkably intensified protein nitration. The organs of *Brassica* species reacted differentially to excess zinc, since in the shoot system modification of the nitration pattern occurred (with newly appeared nitrated protein bands), while in the roots, a general increment in the nitroproteome could be observed (the intensification of the same protein bands being present in the control samples). When we consider the zinc-induced changes of protein nitration in the shoot system, it can be assumed that the significant alteration of its pattern is coupled with enhanced zinc sensitivity, but the zinc-induced general intensification of protein nitration is rather attached to relative zinc endurance.

5. ACKNOWLEDGEMENTS

The research was funded by the Hungarian Scientific Research Fund (Grant no. OTKA PD100504) and Hungary-Serbia IPA Cross-border Co-operation Programme (PLANTTRAIN, HUSRB/1203/221/173). Authors also acknowledge TÁMOP-4.2.2.B-15/1/KONV-2015-0006 project for supporting.

6. REFERENCES

Ambler JE, Brown JC, Gauch HG (1970) Effect of zinc on translocation of iron in soybean plants. *Plant Phys* 46:320–323.

Andreini C, Bertini I (2009) Metalloproteomes: a bioinformatic approach. *Acc Chem Res* 42:1471–1479.

Apel K, Hirt H (2004) Reactive oxygen species: metabolism, oxidative stress, and signal transduction. *Annu Rev Plant Biol* 55:373-399.

Arasimowicz-Jelonek M, Floryszak-Wieczorek J (2011) Understanding the fate of peroxynitrite in plant cells-from physiology to pathophysiology. *Phytochem* 72:681-688.

Baker AJM (1987) Metal tolerance. *New Phytol* 106:93-111.

Bartha B, Kolbert Zs, Erdei L (2005) Nitric oxide production induced by heavy metals in *Brassica juncea* L. Czern. and *Pisum sativum* L. *Acta Biol Szeged* 49:9-12.

Baszynski T, Tukendorf A, Ruszkowska M, Skorzynska E, Maksymiec W (1988) Characteristic of the photosynthetic apparatus of copper non-tolerant spinach exposed to excess copper. *J Plant Physiol* 132:708–713.

Beauchamp C, Fridovich I (1971) Superoxide dismutase: improved assays and an assay applicable to acrylamide gels. *Anal Biochem* 44:276-287.

496 Begara-Morales JC, Chaki M, Sánchez-Calvo B, Mata-Pérez C, Letterier M, Palma JM,
 497 Barroso JB, Corpas FJ (2013) Protein tyrosine nitration in pea roots during development and
 498 senescence. *J Exp Bot* 64:1121-1134.
 499
 500 Bradford MM (1976) A rapid and sensitive method for the quantitation of microgram quantities
 501 of protein utilizing the principle of protein-dye binding. *Anal Biochem* 72:248-254.
 502
 503 Broadley MR, White PJ, Hammond JP, Zelko I, Lux A (2007) Zinc in plants. *New Phytol* 173:
 504 677–702
 505
 506 Chaki M, Valderrama R, Ana M. Fernández-Ocaña AM et al. (2009) Protein targets of tyrosine
 507 nitration in sunflower (*Helianthus annuus* L.) hypocotyls. *J Exp Bot* 60:4221-4234.
 508
 509 Chaki M, Alvarez de Morales P, Ruiz C, Begara-Morales JC, Barroso JB, Corpas FJ, Palma JM
 510 (2015) Ripening of pepper (*Capsicum annuum*) fruit is characterized by an enhancement of
 511 protein tyrosine nitration. *Ann Bot* doi: 10.1093/aob/mcv016.
 512
 513 Chang H-B, Lin C-W, Huang H-J (2005) Zinc-induced cell death in rice (*Oryza sativa* L.) roots.
 514 *Plant Growth Regul* 46:261–266.
 515
 516 Corpas FJ, Chaki M, Fernández- Ocaña A, Valderrama R, Palma JM, Carreras A, Begara-
 517 Morales JC, Airaki M, del Río LA, Barroso JB (2008) Metabolism of reactive nitrogen species
 518 in pea plants under abiotic stress conditions. *Plant Cell Physiol* 49:1711-1722.
 519

520 Corpas FJ, Palma JM, del Río LA, Barroso JB (2013) Protein tyrosine nitration in higher plants
 521 grown under natural and stress conditions. *Front Plant Sci* 4:29.

522

523 Cuypers A, Vangronsveld J, Clijsters H (2002) Peroxidases in roots and primary leaves of
 524 *Phaseolus vulgaris* copper and zinc phytotoxicity: a comparison. *J Plant Physiol* 159:869–876.

525

526 Dhindsa RS, Plumb-Dhindsa P, Thorpe TA (1981) Leaf senescence: correlated with increased
 527 levels of membrane permeability and lipid peroxidation, and decreased levels of superoxide
 528 dismutase and catalase. *J Exp Bot* 32:93–101.

529

530 Di Baccio D, Kopriva S, Sebastiani L, Rennenberg H (2005) Does glutathione metabolism have
 531 a role in the defence of poplar against zinc excess? *New Phytol* 167:73–80.

532

533 Ebbs S, Uchil S (2008) Cadmium and zinc induced chlorosis in Indian mustard [*Brassica juncea*
 534 (L.) Czern] involves preferential loss of chlorophyll b. *Photosynth* 46:49-55.

535

536 Ebbs SD, Kochian LV (1997) Toxicity of zinc and copper to *Brassica* species: implications for
 537 phytoremediation. *J Environ Qual* 26:776-781.

538

539 Ebbs SD, Lasat MM, Brady DJ, Cornish J, Gordon R, Kochian LV (1997) Phytoextraction of
 540 cadmium and zinc from a contaminated soil. *J Environ Qual* 26:1424-1430.

541

542 Feigl G, Kumar D, Lehotai N, Tugyi N, Molnár Á, Ördög A, Szepesi Á, Gémes K, Laskay G,
 543 Erdei L, Kolbert Zs (2013) Physiological and morphological responses of the root system of

544 Indian mustard (*Brassica juncea* L. Czern.) and rapeseed (*Brassica napus* L.) to copper stress.
 545 Ecotoxicol Environ Safety 94:179-189.
 546
 547 Fraústo da Silva JJR, Williams RJP (2001) The Biological Chemistry of the Elements, 2nd edn.
 548 Clarenton Press, Oxford, UK.
 549
 550 Galetskiy D, Lohscheider JN, Kononikhin AS, Popov IA, Nikolaev EN, Adamska I (2011)
 551 Phosphorylation and nitration levels of photosynthetic proteins are conversely regulated by
 552 light stress. Plant Mol Biol 77:461-473.
 553
 554 Godbold DL, Huttermann A (1985) Effect of zinc, cadmium and mercury on root elongation of
 555 *Picea abies* (Karst.) seedlings, and the significance of these metals to forest die-back. Environ
 556 Pollut 38A:375–381.
 557
 558 Gow AJ, Farkouh CR, Munson DA, Posencheg MA, Ischiropoulos H (2004) Biological
 559 significance of nitric oxide-mediated protein modifications. Am J Physiol Lung Cell Mol
 560 Physiol 287:L262-L268.
 561
 562 Heath R, Packer L (1968) Photoperoxidation in isolated chloroplasts. I. Kinetics and
 563 stoichiometry of fatty acid per-oxidation. Arch Biochem Biophys 196:385–395.
 564
 565 Jain R, Srivastava S, Solomon S, Shrivastava AK, Chandra A (2010) Impact of excess zinc on
 566 growth parameters, cell division, nutrient accumulation, photosynthetic pigments and oxidative
 567 stress of sugarcane (*Saccharum* spp.). Acta Physiol Plant 32:979–986.
 568

569 Kolbert Zs, Pető A, Lehotai N, Feigl G, Ördög A, Erdei L (2012) *In vivo* and *in vitro* studies on
570 fluorophore-specificity. *Acta Biol Szeged* 56:37-41.

571

572 Krupa Z, Baszynski T (1995) Some aspects of heavy metals toxicity towards photosynthetic
573 apparatus - direct and indirect effects on light and dark reactions. *Acta Physiol Plant* 7:55-64.

574

575 Kumar PBAN, Dushenkov V, Motto H, Raskin I (1995) Phytoextraction: The use of plants to
576 remove heavy metals from soils. *Environ Sci Technol* 29:1232-1238.

577

578 Kupper H, Kupper F, Spiller M (1996) Environmental relevance of heavy metal-substituted
579 chlorophylls using the example of water plants. *J Exp Bot* 47:259-266.

580

581 Last PJ, Bean MR (1991) Controlling manganese deficiency in sugarbeet with foliar sprays. *J*
582 *Agri Sci* 116:351-358.

583

584 Lehotai N, Kolbert Zs, Pető A, Feigl G, Ördög A, Kumar D, Tari I, Erdei L (2012) Selenite-
585 induced hormonal and signalling mechanisms during root growth of *Arabidopsis thaliana* L. *J*
586 *Exp Bot* 15:5677-5687.

587

588 Li X, Yang Y, Jia L, Chen H, Wei X (2013) Zinc-induced oxidative damage, antioxidant
589 enzyme response and proline metabolism in roots and leaves of wheat plants. *Ecotoxicol*
590 *Environ Safety* 89:150–157.

591

592 Lichtenthaler HK (1987) Chlorophylls and carotenoids: pigments of photosynthetic
593 biomembranes. *Meth Enzymol* 148:350–382.

594

595 Lu L, Tian S, Zhang J et al. (2013) Efficient xylem transport and phloem remobilization of Zn
 596 in the hyperaccumulator plant species *Sedum alfredii*. *New Phytol* 198:721–731.

597

598 Misra A, Ramani S (1991) Inhibition of iron absorption by zinc-induced iron deficiency in
 599 Japanese mint. *Acta Physiol Plant* 13:37-42.

600

601 Monnet F, Vaillant N, Vernay P, Coudret A, Sallanon H, Hitmi A (2001) Relationship between
 602 PSII activity, CO₂ fixation, and Zn, Mn and Mg contents of *Lolium perenne* under zinc stress.
 603 *J Plant Physiol* 158:1137-1144.

604

605 Morina F, Jovanovic L, Mojovic M, Vidovic M, Pankovic D, Sonja Veljovic Jovanovic S
 606 (2010) Zinc-induced oxidative stress in *Verbascum thapsus* is caused by an accumulation of
 607 reactive oxygen species and quinhydrone in the cell wall. *Physiol Plant* 140:209–224.

608

609 Munzuroglu O, Geckil H (2002) Effects of metals on seed germination, root elongation, and
 610 coleoptile and hypocotyl growth in *Triticum aestivum* and *Cucumis sativus*. *Arch Environ*
 611 *Contam Toxicol* 43:203–213.

612

613 Nakano Y, Asada K (1981) Hydrogen peroxide is scavenged by ascorbate specific peroxidase
 614 in spinach chloroplasts. *Plant Cell Physiol* 22:867-880.

615

616 Nieboer E, Richardson DHS (1980) The replacement of the nondescript term ‘heavy metal’ by
 617 a biologically significant and chemically significant classification of metal ions. *Environ Pollut*
 618 *B*1:3–26.

619

620 Potters G, Pasternak TP, Guisez Y, Jansen MA (2009) Different stresses, similar morphogenic
 621 responses: integrating a plethora of pathways. *Plant Cell Environ* 32:158-169.

622

623 Prasad MNV, Strzalka K, (1999) Impact of heavy metals on photosynthesis. In: Prasad, M.N.V.,
 624 Hagemeyer, J. (Eds.), *Heavy Metal Stress in Plants: from Molecules to Ecosystems*. Springer,
 625 Berlin, pp. 117–138.

626

627 Roháček K, Soukupová J, Barták M (2008) Chlorophyll fluorescence: A wonderful tool to study
 628 plant physiology and plant stress. In: Benoît Schoefs (ed) *Plant Cell Compartments - Selected*
 629 *Topics, Research Signpost, Fort P.O., Trivandrum-695 023, Kerala*, pp 41-104.

630

631 Rout GR, Das P (2003) Effect of metal toxicity on plant growth and metabolism: I. Zinc. *Agro-*
 632 *Sci Product Vegetal l'Environ* 23:3-12.

633

634 Schützendübel A, Polle A (2002) Plant responses to abiotic stresses: heavy metal-induced
 635 oxidative stress and protection by mycorrhization. *J Exp Bot* 53:1351-1365.

636

637 Shi GR, Cai QS (2009) Photosynthetic and anatomic responses of peanut leaves to zinc stress.
 638 *Biol Plant* 53:391-394.

639

640 Sinha P, Jain R, Chatterjee C (2000) Interactive effect of boron and zinc on growth and
 641 metabolism of mustard. *Comm Soil Sci Plant Anal* 31:41–49.

642

643 Smith JM, Dasgupta TP (2000) Kinetics and mechanism of the decomposition of S-
644 nitrosoglutathione by ascorbic acid and copper ions in aqueous solution to produce nitric oxide.
645 Nitric Oxide 4:57-66.

646

647 Stoyanova Z, Doncheva S (2002) The effect of zinc supply and succinate treatment on plant
648 growth and mineral uptake in pea plant. Braz J Plant Physiol 14:111-116.

649 Teige M, Huchzermeyer B, Schultz G (1990) Inhibition of chloroplast ATPsynthase/ATPase is
650 a primary effect of heavy metal toxicity in spinach plants. Biochem Physiol Pfl 186:165-168.

651

652 Tewari RK, Kumar P, Sharma PD (2008) Morphology and physiology of zinc-stressed
653 mulberry plants. J Plant Nutr Soil Sci 171:286-294.

654

655 Van Assche F Clijsters H (1986) Inhibition of photosynthesis in *Phaseolus vulgaris* by
656 treatment with toxic concentration of zinc: effect on ribulose-1,5-biphosphate
657 carboxylase/oxygenase. J Plant Physiol 125:355-360.

658

659 van de Mortel JE, Villanueva LA, Schat H, Kwekkeboom J, Coughlan S, Moerland PD, Aarts,
660 MG (2006) Large expression differences in genes for iron and zinc homeostasis, stress
661 response, and lignin biosynthesis distinguish roots of *Arabidopsis thaliana* and the related metal
662 hyperaccumulator *Thlaspi caerulescens*. Plant Phys 142:1127-1147.

663

664 van der Vliet A, Eiserich JP, Shigenana MK, Cross CE (1999) Reactive nitrogen species and
665 tyrosine nitration in the respiratory tract: epiphenomena or a pathobiologic mechanism of
666 disease? Am J Respir Crit Care Med 160:1-9.

667

668 Wang C, Zhang SH, Wang PF, Hou J, Zhang WJ, Li W, Lin ZP (2009) The effect of excess Zn
669 on mineral nutrition and antioxidative response in rapeseed seedlings. *Chemosphere* 75:1468–
670 1476.

671

672 White MC, Baker FD, Chaney RL, Decker AM (1981) Metal complexation in xylem fluid. II.
673 Theoretical equilibrium model and computational computer program. *Plant Phys* 67:301-310.

674

675 Xu J, Yin H, Li Y, Liu X (2010) Nitric oxide is associated with long-term zinc tolerance in
676 *Solanum nigrum*. *Plant Phys* 154:1319-1334.

677

678 Yang, Z-Y, Chen F-H, Yuan J-G, Zheng Z-W, Wong M-H (2004) Responses of *Sesbania*
679 *rostrata* and *S. cannabina* to Pb, Zn, Cu and Cd toxicities. *J Environ Sci* 16:670–673.

680

681 Zarcinas BA, Ishak CF, McLaughlin MJ, Cozens G (2004) Heavy metals in soils and crops in
682 Southeast Asia. *Environ Geochem Health* 26:343-357.

683

Figures and figure legends

Fig 1 Concentration of zinc ($\mu\text{g/g}$ dry weight) in the root (a) and shoot (b) system of 0, 50, 150 or 300 μM ZnSO_4 -treated *B. juncea* (●) and *B. napus* (○). Different letters indicate significant differences according to Duncan-test ($n=6$, $P\leq 0.05$)

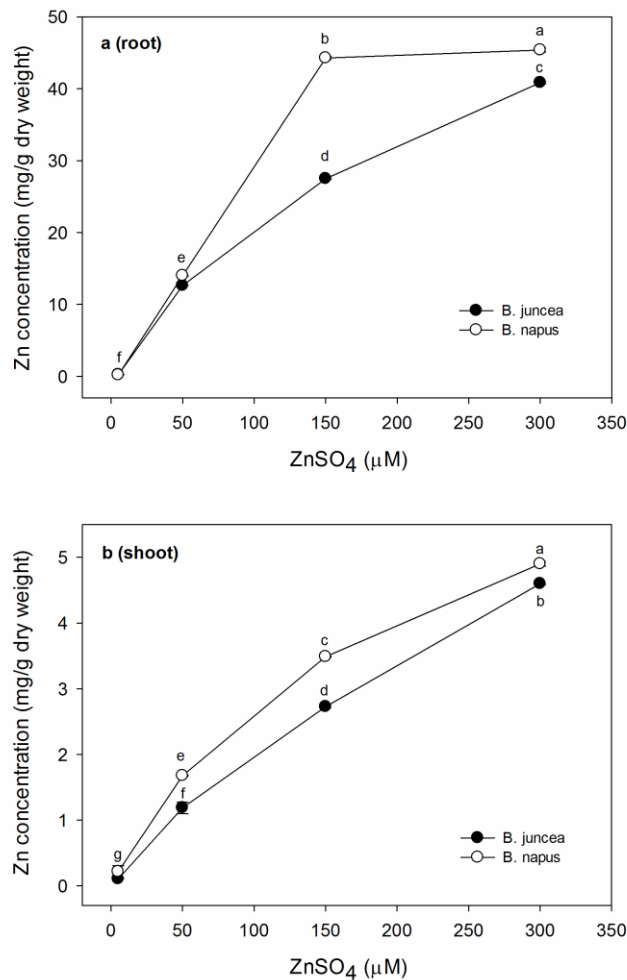


Fig 2 (a) Dry and fresh weight (g) of the shoot system of *Brassica* species treated with 0, 50, 150 or 300 μM Zn. (b) Leaf area (cm^2) of control and Zn-exposed *Brassica* plants. Different letters indicate significant differences according to Duncan-test ($n=20$, $P\leq 0.05$). (c) Photographs taken from the shoot system of control and 300 μM Zn-treated *B. juncea* and *B.*

693 *napus*. Bar=30 cm. (d) Representative photographs of *Brassica* leaves demonstrating the effect
 694 of zinc concentrations on morphology and on the appearance of chlorosis and necrosis (marked
 695 by white arrows). Bar=5 cm

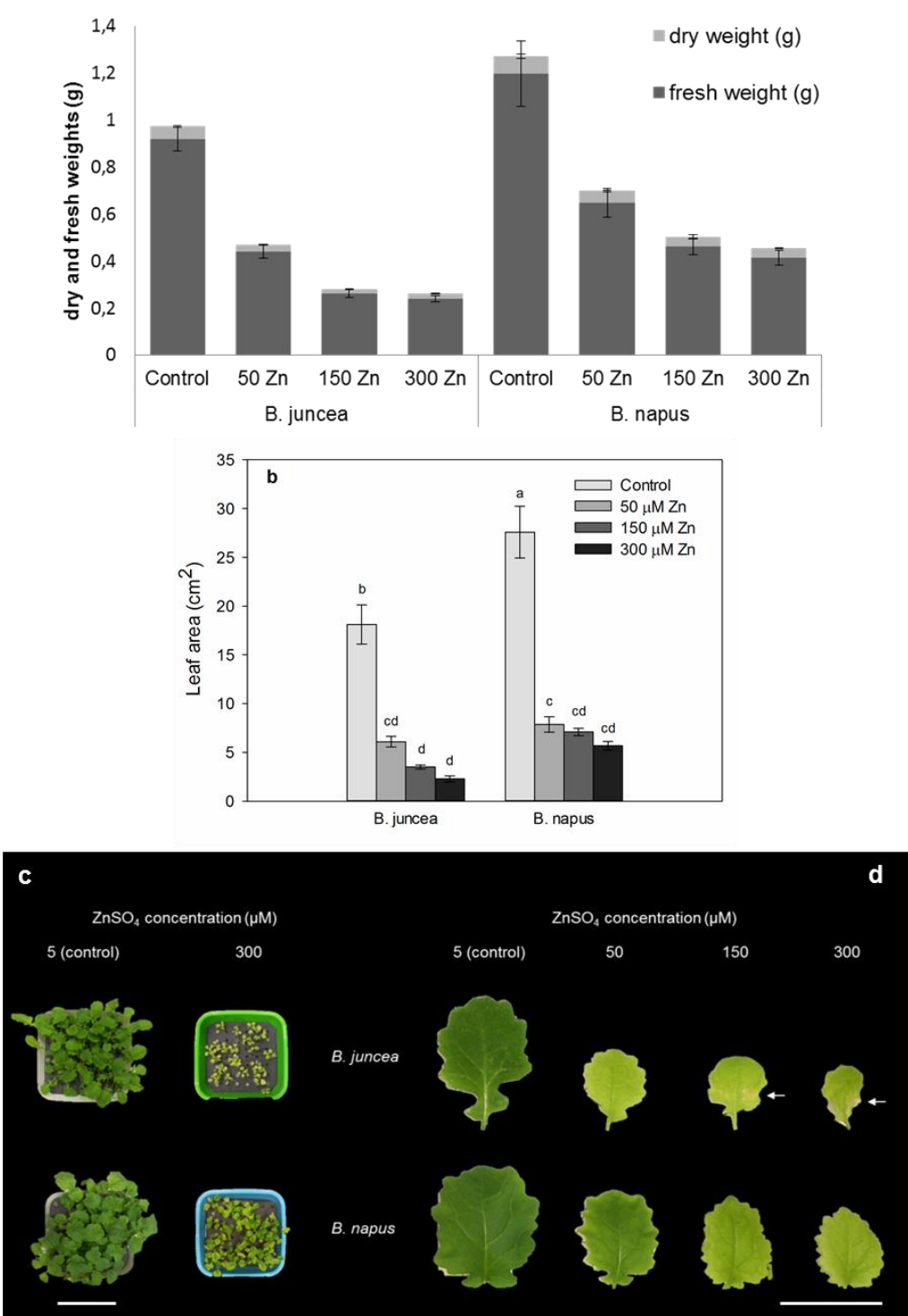


Fig 3 Chlorophyll fluorescence parameters (Yield, ETR, qP, NPQ) of *B. juncea* (a) and *B. napus* (b) leaves after 14-days-long zinc exposure

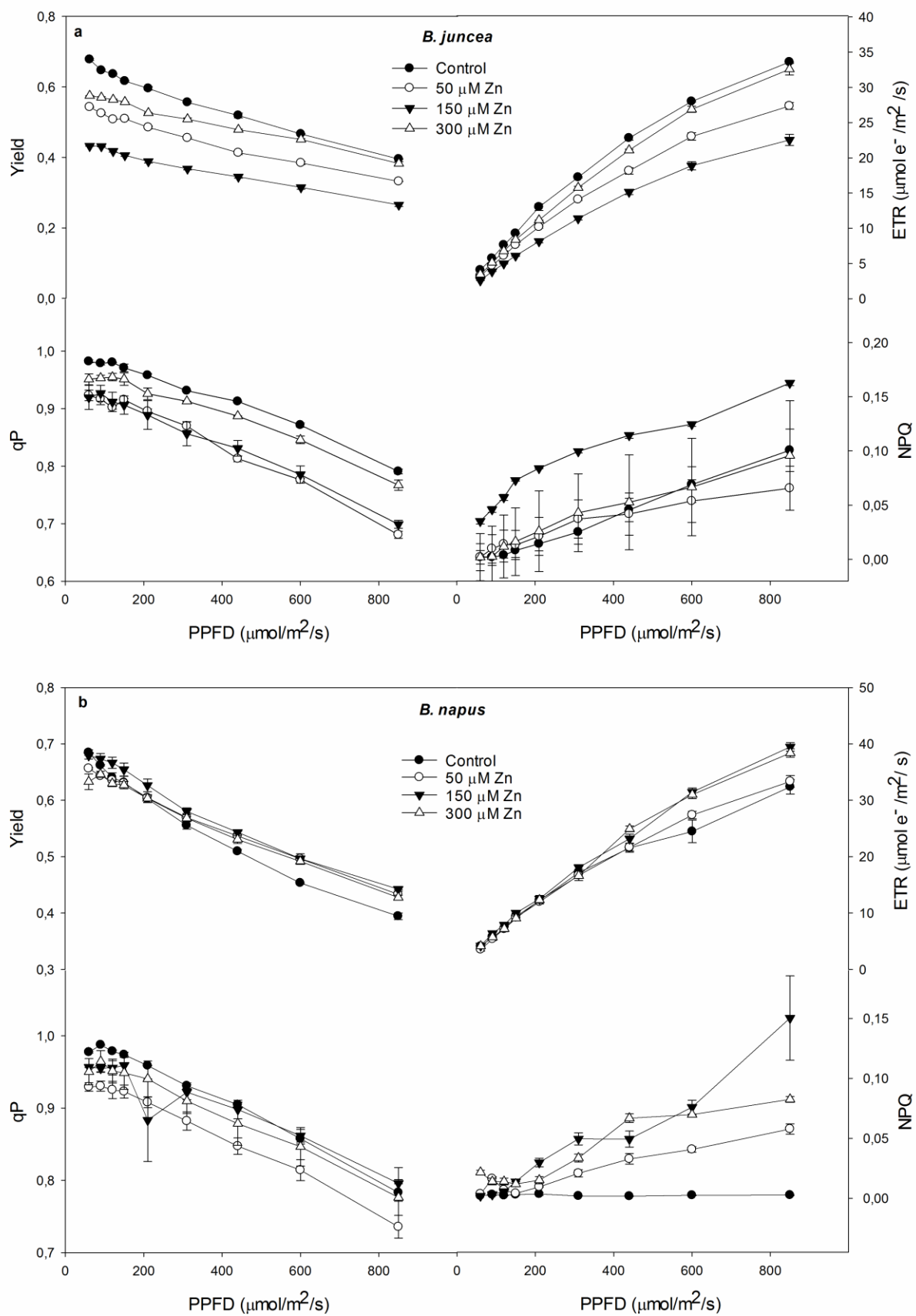


Fig 4 (a) Dry and fresh weight (g) of the root system of *Brassica* species treated with 0, 50, 150 or 300 μM Zn. Length of the primary (b) and the lateral (c) roots and the number of lateral roots (d) in control and Zn-exposed *Brassica* species. (e) Viability of the root meristem cells (pixel intensity of fluorescein, control%) of control and Zn-treated *Brassica* species. Different letters indicate significant differences according to Duncan-test ($n=10-20$, $P\leq 0.05$)

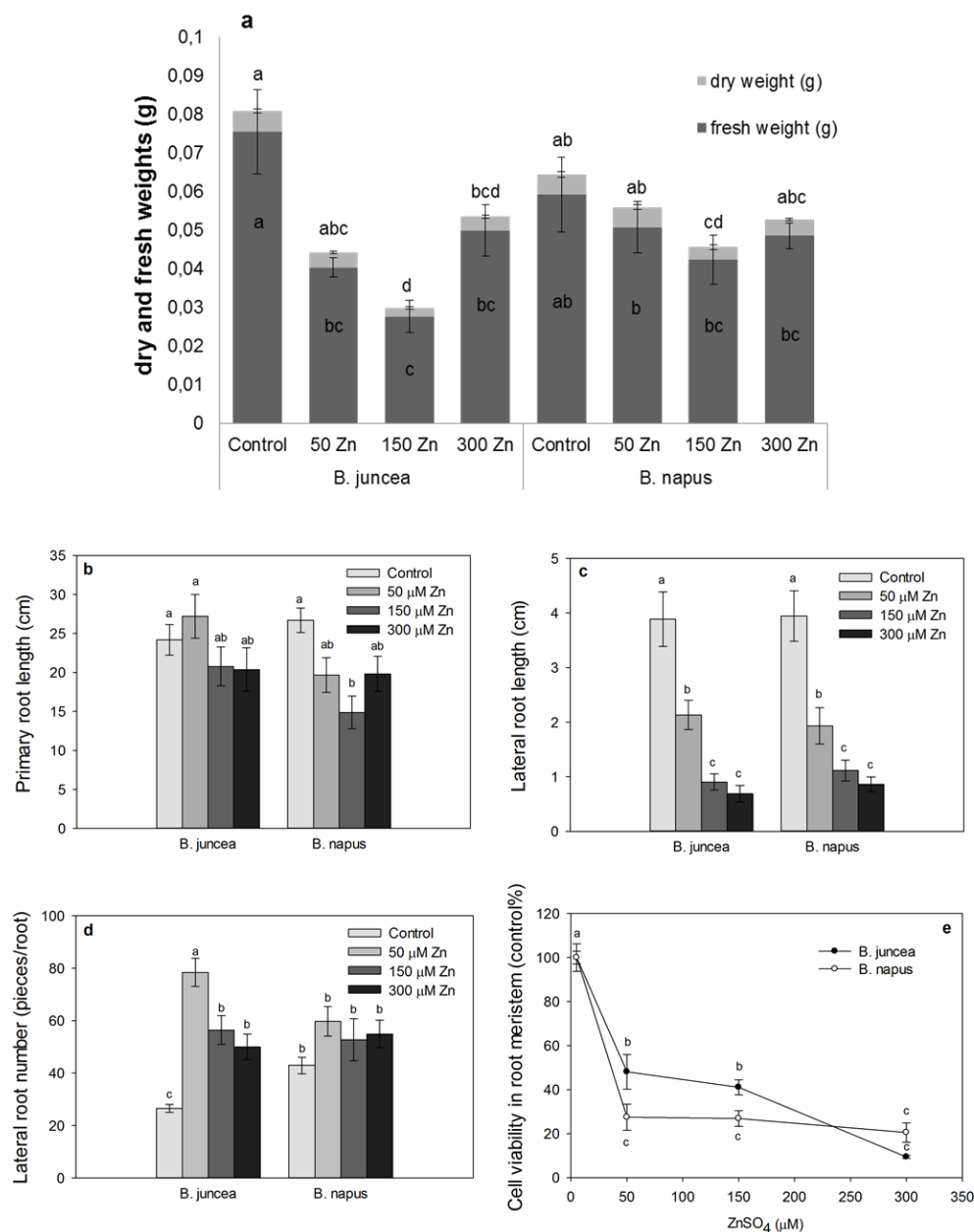


Fig 5 The level of superoxide anion (pixel intensity of DHE, a), hydrogen peroxide (pixel intensity of resorufin, b), nitric oxide (pixel intensity of DAF FM, c) and peroxynitrite (pixel

intensity of APF, d) in the root meristem of 0, 50, 150 or 300 μM Zn-exposed *B. juncea* and *B. napus*. Different letters indicate significant differences according to Duncan-test ($n=10-15$, $P\leq 0.05$). (e) Representative microscopic images of control and 150 μM Zn-treated *Brassica napus* root tips: DHE, DAF-FM, APF. Bar=0.5 mm

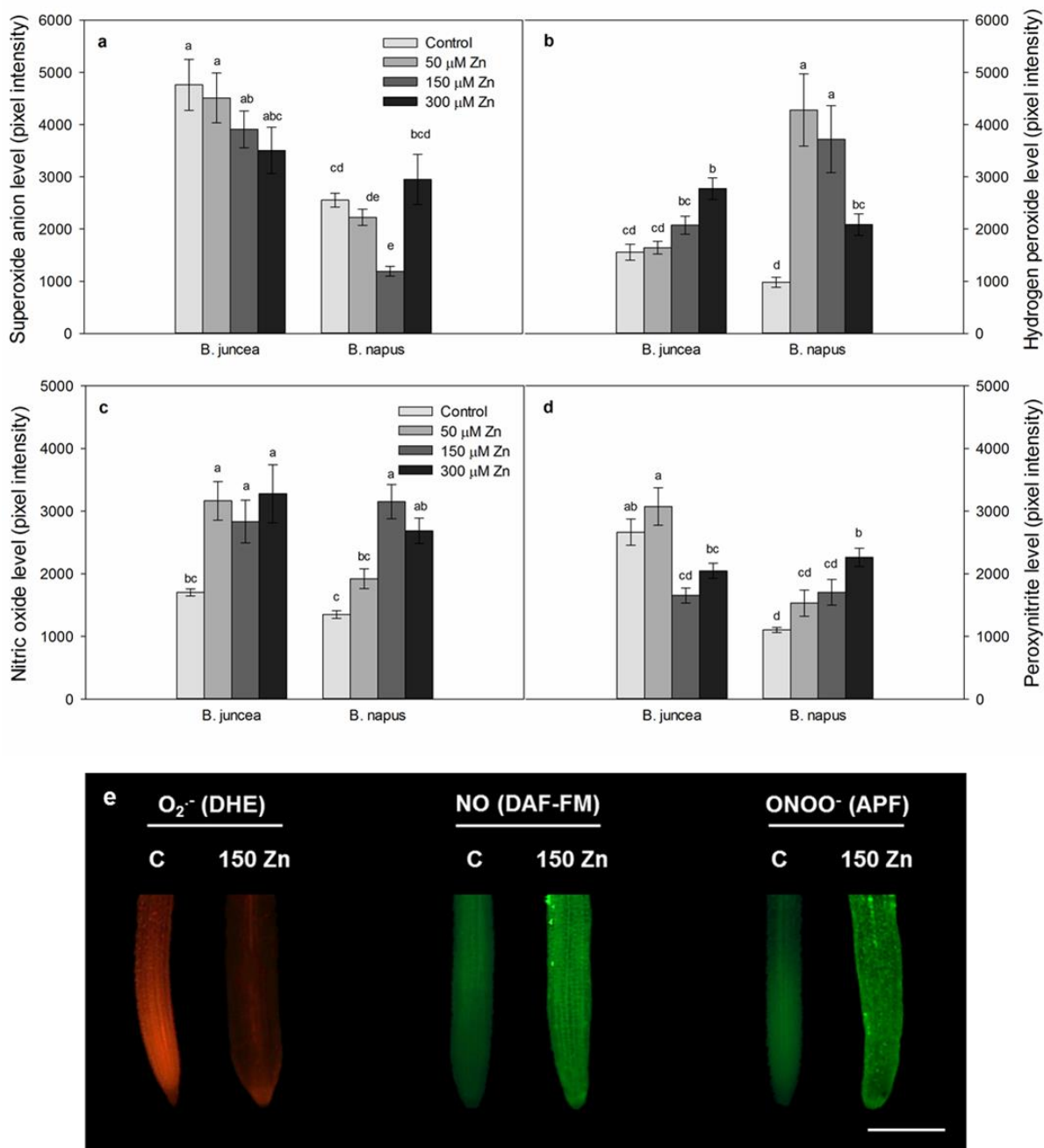


Fig 6 Activity of SOD (unit/g fresh weight, a) enzyme and the analysis of SOD isoforms in the shoot and root of *B. napus* and *B. juncea* (b). SOD isoforms were separated by native-PAGE

and stained by a photochemical method using 30 µg of protein per lane. Activity of APX (unit/g
 fresh weight, c) in the shoot and root system of *Brassica* species treated with 0, 50, 150 or 300
 µM Zn. (d) Concentration of TBARS (nmol/g fresh weight) in the shoot and root of control and
 Zn-treated *Brassica* species. Different letters indicate significant differences according to
 Duncan-test (n=6, P≤0.05)

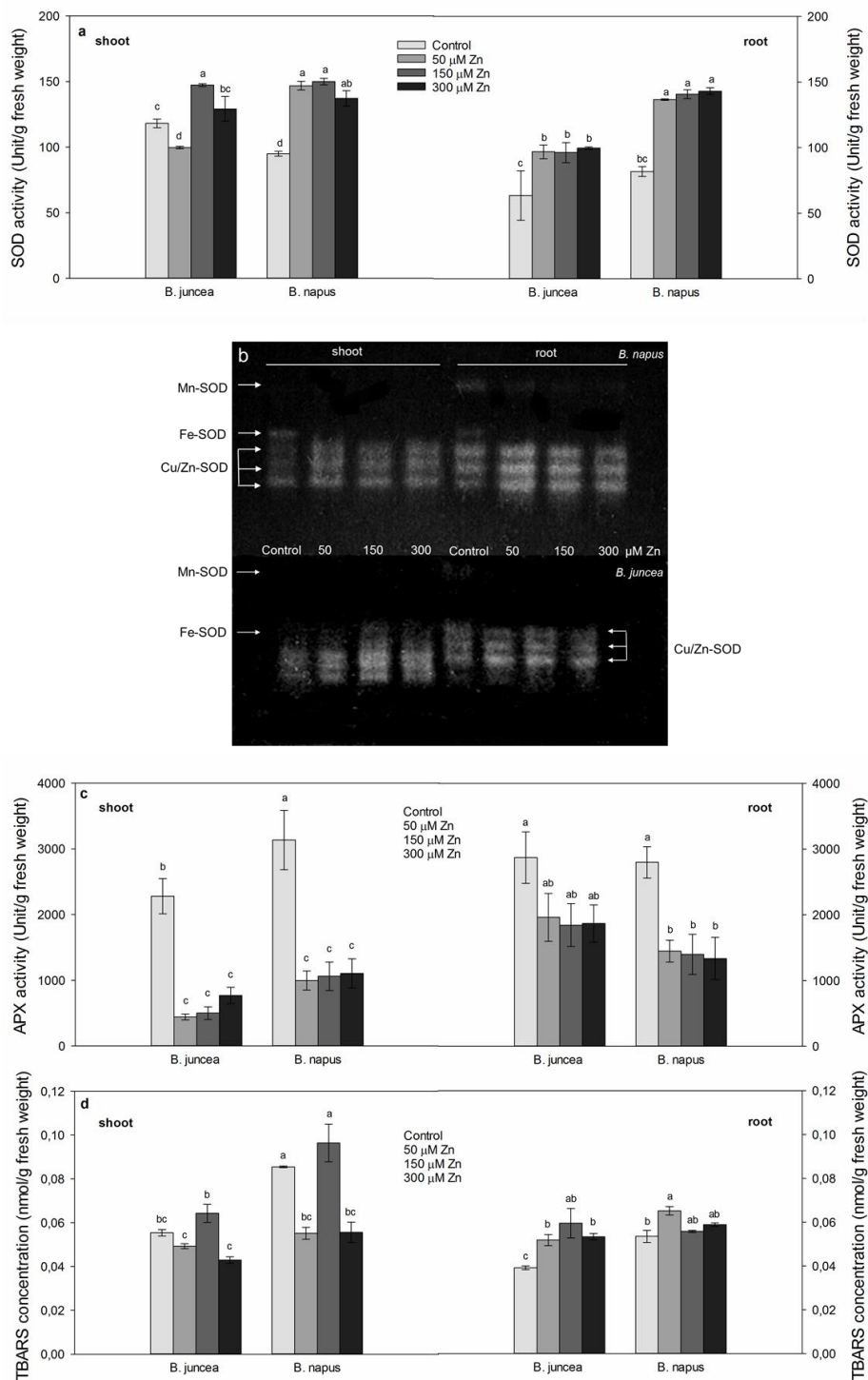
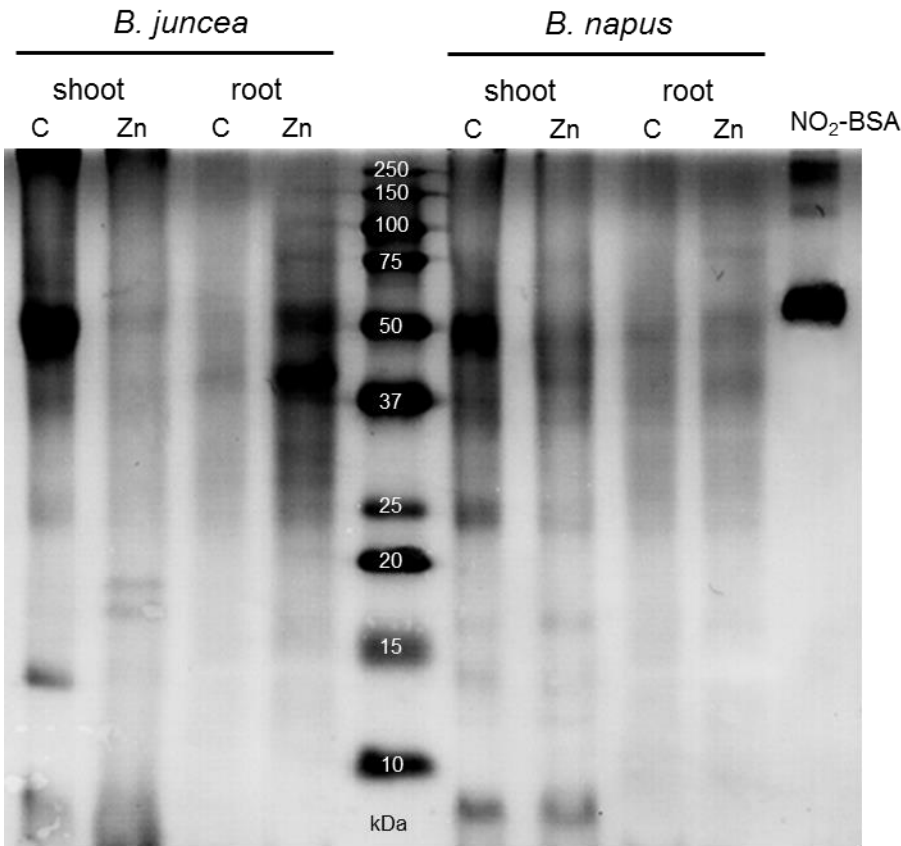
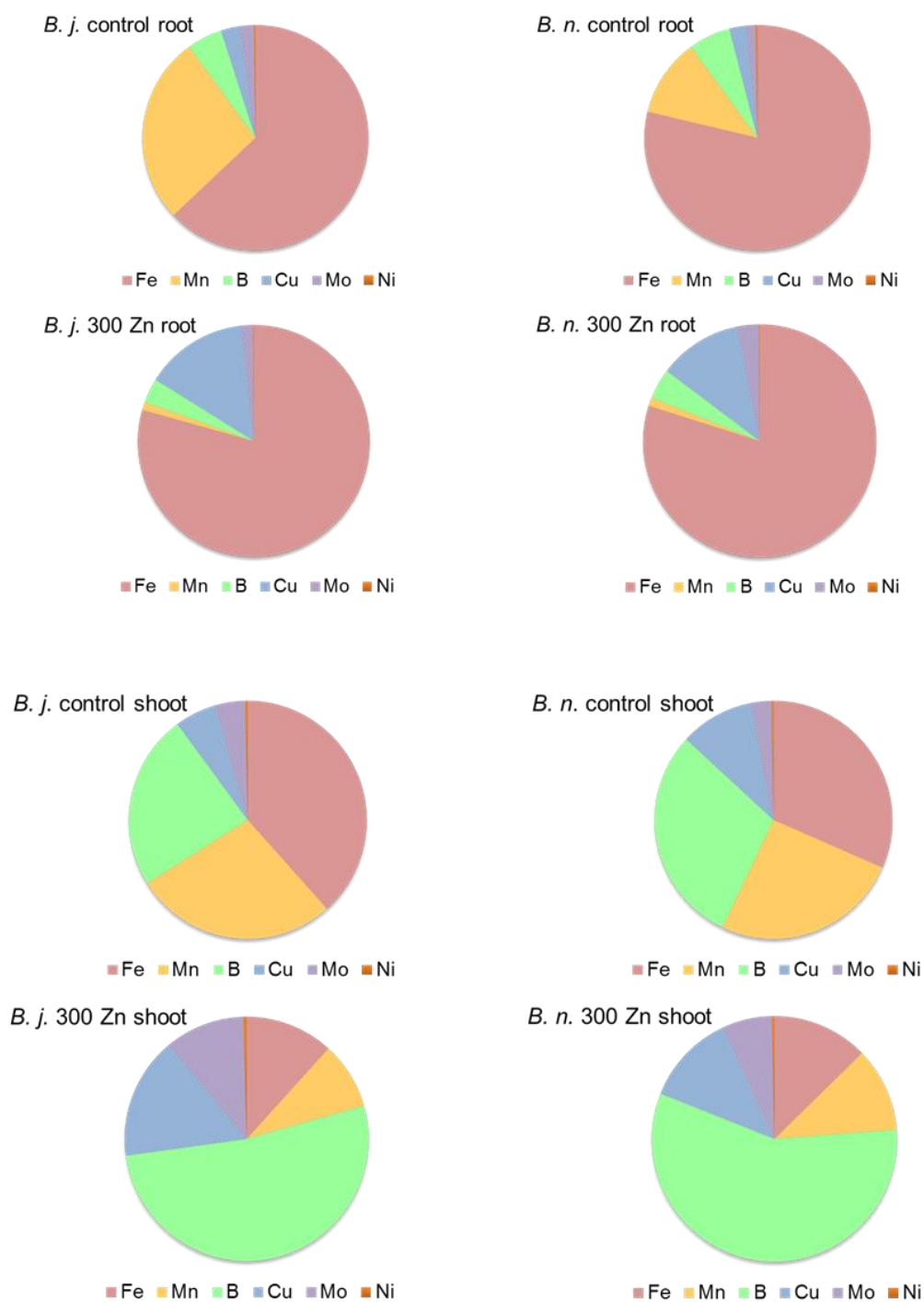


Fig 7 Representative immunoblots showing protein tyrosine nitration in roots and shoots of *B. juncea* and *B. napus* plants under control conditions (C) and during 150 μ M Zn exposure (Zn). Root and shoot samples were separated by SDS-PAGE and analysed on Western blotting with anti-nitrotyrosine antibody (1:2000). Commercial nitrated BSA (NO₂-BSA) was used as a positive control



Supplementary Figure 1 Ratios of different microelement (Fe, Mn, B, Cu, Mo, Ni) concentrations (μ g/g dry weight) in the shoot and root system of control and 300 μ M Zn-exposed *Brassica juncea* (*B. j.*) and *Brassica napus* (*B. n.*)



Supplementary Table 1 Concentration of photosynthetic pigments ($\mu\text{g/g}$ FW) and the Chl *a/b* ratios in the leaves of control and Zn-treated *B. juncea* and *B. napus*. Different letters indicate significant differences according to Duncan-test ($n=6$, $P\leq 0.05$)

735 **Supplementary Table 1** Concentration of photosynthetic pigments ($\mu\text{g/g}$ FW) and the Chl *a/b*
736 ratios in the leaves of control and Zn-treated *B. juncea* and *B. napus*. Different letters indicate
737 significant differences according to Duncan-test (n=6, $P \leq 0.05$)

738

		Chl a	Chl b	Chl a/b	Total chl	Carotenoids
B. juncea	Control	19.00 \pm 0.52 ^a	4.99 \pm 0.68 ^a	3.04 ^a	20.18 \pm 1.21 ^a	4.2 \pm 0.05 ^a
	50 Zn	4.05 \pm 0.52 ^b	1.57 \pm 0.76 ^b	2.56 ^b	5.63 \pm 1.28 ^b	1.10 \pm 0.07 ^b
	150 Zn	3.37 \pm 0.42 ^b	1.6 \pm 0.82 ^b	2.09 ^b	4.97 \pm 1.24 ^b	0.9 \pm 0.10 ^c
	300 Zn	2.05 \pm 0.49 ^c	1.15 \pm 0.8 ^b	1.77 ^b	3.21 \pm 1.34 ^b	0.40 \pm 0.13 ^d
B. napus	Control	21.65 \pm 0.05 ^a	5.31 \pm 1.24 ^a	4.07 ^a	26.97 \pm 1.19 ^a	6.73 \pm 0.25 ^a
	50 Zn	11.92 \pm 0.13 ^b	2.03 \pm 1.17 ^b	5.86 ^b	13.93 \pm 1.04 ^b	4.35 \pm 0.71 ^b
	150 Zn	4.06 \pm 0.48 ^c	1.71 \pm 0.86 ^b	2.36 ^c	5.78 \pm 1.3 ^c	1.14 \pm 0.11 ^c
	300 Zn	4.30 \pm 0.59 ^c	0.75 \pm 0.29 ^b	5.86 ^b	5.06 \pm 0.88 ^c	1.38 \pm 0.10 ^c

739